

# 1 Test of the equivalence principle with antihydrogen

The goal of the AEGIS experiment (CERN/AD6) is to test the Weak Equivalence Principle (WEP) using antihydrogen ( $\bar{H}$ ) with a precision of 1% on the gravitation acceleration  $\bar{g}$ . This principle of the universality of free fall has been tested with high precision for matter, but not with antimatter, due to major technical difficulties related to stray electric and magnetic fields. In contrast, the electrically neutral  $\bar{H}$  atom is an ideal probe to test the WEP, and the antiproton decelerator (AD) at CERN is a worldwide unique antihydrogen factory. In AEGIS the gravitational deflection of  $\bar{H}$  atoms launched horizontally and traversing a moiré deflectometer can be measured with a precision of 1% on  $|\Delta g|/g$ , using a position sensitive antihydrogen detector. Details on the experiment can be found in ref. [1, 2].

However, achieving the 1% goal requires antihydrogen temperatures in the sub-K range and correspondingly an intensive R&D, which will be continued during the 2019-2020 long shutdown of the CERN accelerators. Hence AEGIS plans to start measurements of  $\bar{g}$  with the experiment transferred to the Extremely Low Energy Antiproton Ring (ELENA) ring. Realistically, one can expect first data on  $\bar{g}$  from AEGIS to be available in 2022. This report describes some of our antihydrogen detector developments to measure accurately the annihilation point of antihydrogen behind the deflectometer (section 1.1), and to characterize the antihydrogen cloud at the production point (section 1.2).

In the original proposal [1] a resolution of some 10  $\mu\text{m}$  was to be achieved with a silicon strip annihilation detector. In 2012 we tested a new idea to instead use emulsion films to achieve a resolution of the order of 1  $\mu\text{m}$  [3, 4], and completed the construction of the annihilation detector (FACT) to characterize the antihydrogen cloud prior to its acceleration into an  $\bar{H}$  beam. Fig. 1.1 shows the status of the AEGIS apparatus in 2012.

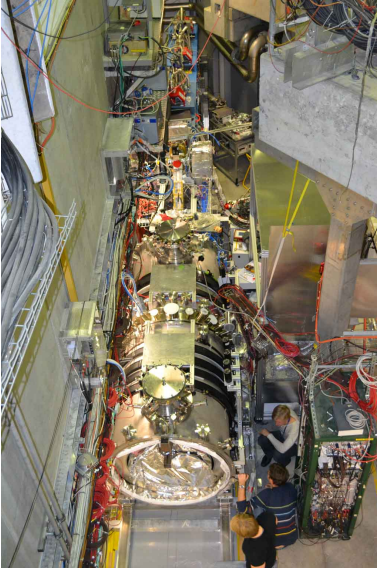


Figure 1.1: *Picture of the AEGIS apparatus in the AD-hall at CERN in December 2012.*

## 1.1 Nuclear emulsions to measure $g$ with antihydrogen

Nuclear emulsions [5] are photographic films with extremely high spatial resolution. A track produced by a charged particle is detected as a sequence of silver grains, where about 36 Ag grains per 100  $\mu\text{m}$  are created by a minimum ionizing particle. The intrinsic spatial resolution is around 50 nm. For AEGIS the AEC-Bern group developed nuclear emulsions which can be used in ordinary vacuum (OVC,  $10^{-5} - 10^{-7}$  mbar). Fig. 1.2 (left) shows the setup envisaged for the  $\bar{g}$ -measurement. The

expected performance is also shown: the number of antihydrogen annihilations required to achieve a given precision decreases dramatically with improving resolution.

A sketch of the setup used for test exposures with stopping antiprotons in 2012 is shown in fig. 1.2 (right). The emulsion detector consisted of 5 sandwiches made of emulsion films (OPERA type) deposited on both sides of (200  $\mu\text{m}$  thick) plastic substrates (68 x 68 x 0.3  $\text{mm}^3$ ). A thin foil will be needed in the  $\bar{g}$ -measurement as a window to separate the  $\bar{H}$  beam line at UHV pressure from the OVC section containing the emulsion detector. Thus for the tests half of the emulsion surface was covered by a 20  $\mu\text{m}$  (SUS) stainless steel foil, while direct annihilation on the emulsion surface could be investigated from the other half.

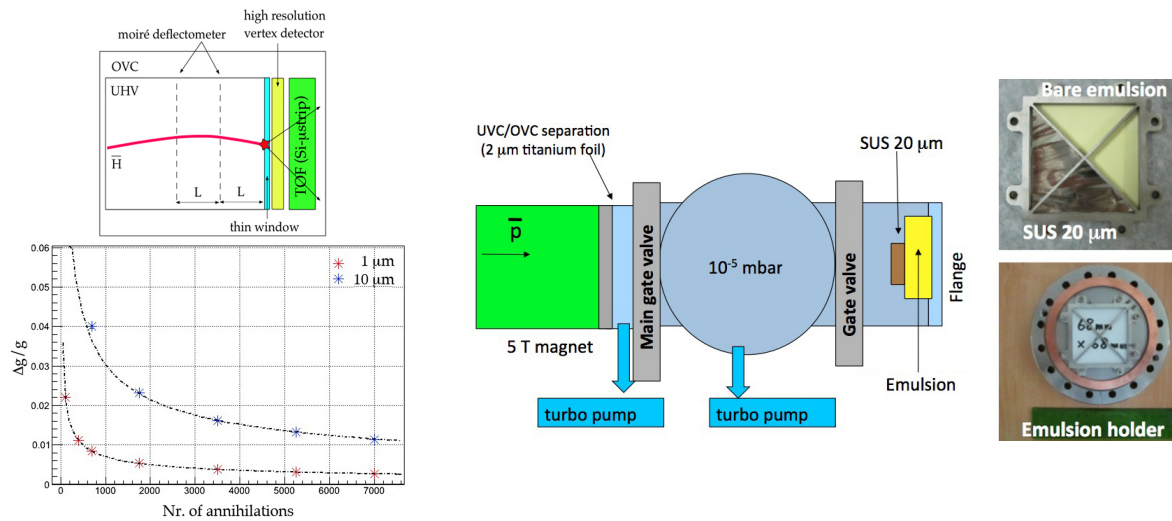


Figure 1.2: Left: schematics of the AEGIS detectors. The vertex detector is made of nuclear emulsions. The time-of-flight detector (TOF) is needed to measure the velocities of the  $\bar{H}$  atoms. Bottom:  $\Delta g/g$  vs. number of particles for a vertex resolution of 1  $\mu\text{m}$  (red) and 10  $\mu\text{m}$  (blue). Right: test setup with a picture of the vacuum flange holding the emulsion stack attached by a crossed bar frame.

In December 2012 the AEC-Bern group also carried out measurements with a series of thin foils of varying compositions (Al, Si, Ti, Cu, Ag, Au, Pb) to determine the relative contributions from protons, nuclear fragments and pions as a function of atomic number. Fig. 1.3 (left) shows annihilation vertices on the bare emulsion surfaces and tracks behind a 5  $\mu\text{m}$  thick silver foil. Tracks emerging from the annihilation vertex are clearly observed. Tracks from nuclear fragments, protons, and pions were reconstructed and the distance of closest approach between pairs of tracks was calculated. Fig. 1.3 (right) shows the distribution of the distance of closest approach projected into the vertical direction (impact parameter), which is a measure of the resolution with which the annihilation point will be determined in the  $g$ -measurement. The figure shows that with e.g. a 20  $\mu\text{m}$  steel window a resolution of  $\simeq 1 \mu\text{m}$  on the vertical position of the annihilation vertex can be achieved.

We have tested the properties of nuclear emulsions in vacuum [3] which, to our knowledge, had not been studied before. Water loss in the gelatine which surrounds the AgBr crystals produces cracks in the emulsion layer, thus compromising the mechanical stability (required at the  $\mu\text{m}$  level). We therefore developed a treatment with glycerine to prevent the elasticity loss in the emulsion. However, glycerine treatment changes the composition of the emulsion layer and we thus had to determine the detection efficiency per AgBr crystal. This was performed with minimum ionizing pions in a 6 GeV/c CERN beam. The result (fig. 1.4) does not indicate any changes in the efficiency, which is typically

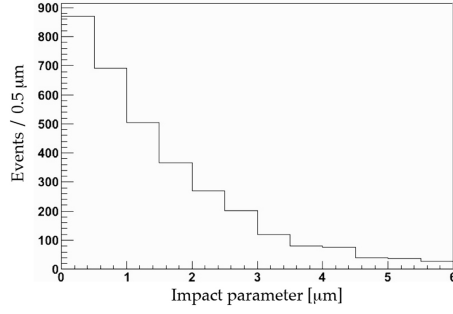
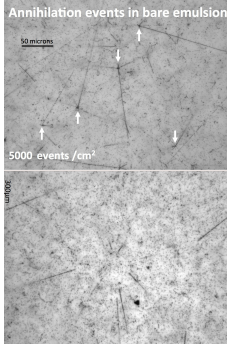


Figure 1.3: *Left: typical antiproton annihilation vertices in the bare emulsion (top) and tracks observed behind a thin silver foil in which the antiprotons annihilate (bottom). Right: impact parameter resolution with a 20  $\mu\text{m}$  stainless steel window.*

13% for glycerine concentrations below 20%. However, the thermally induced background – the so-called fog density – increases for glycerine treated emulsions.

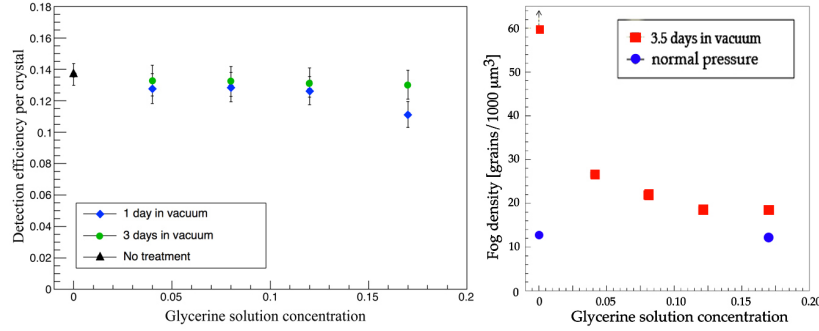


Figure 1.4: *Left: Crystal sensitivity vs. glycerine concentration. Right: Fog density (number of noise grains per  $10^3 \mu\text{m}^3$ ) vs. glycerine concentration for films kept in vacuum for 3.5 days (squares), compared films kept at atmospheric pressure (dots).*

Annihilation products from annihilating antiprotons (or  $\bar{H}$  atoms) are emitted isotropically, in contrast to the  $\tau$ -decay products measured in the OPERA experiment, which are forward boosted. The efficiency of the automatic scanning system available in Bern needs therefore to be improved for tracks traversing the emulsion layers at large incident angles. We are also investigating new emulsion gels with higher sensitivity to increase the detection efficiency for minimum ionizing particles. They were developed at Nagoya University (Japan) and coated onto glass substrates in Bern. Glass is well suited for highest position resolutions thanks to its superior environmental stability (temperature and humidity), as compared to plastic.

A proof of principle of the deflectometer to be used AEGIS was performed in 2012 with emulsion films irradiated with antiprotons passing through a small moiré deflectometer provided by the University of Heidelberg. A photograph of the deflectometer is shown in fig. 1.5 (left). The device contained several pairs of gratings with different spacings, as well as gratings in direct contact with the films. Fig. 1.5 (right) shows the intensity pattern on along the vertical axis. A relative shift between moiré and Talbot-Lau pattern (obtained with light) indicates that a force is present. The observed mean shift of  $9.8 \mu\text{m}$  is consistent with a mean force of 530 aN produced by the Lorentz force from the fringe magnetic field of the AEGIS apparatus (about  $10^{-3}$  T at the position of the deflectometer). Details can be found in [6].

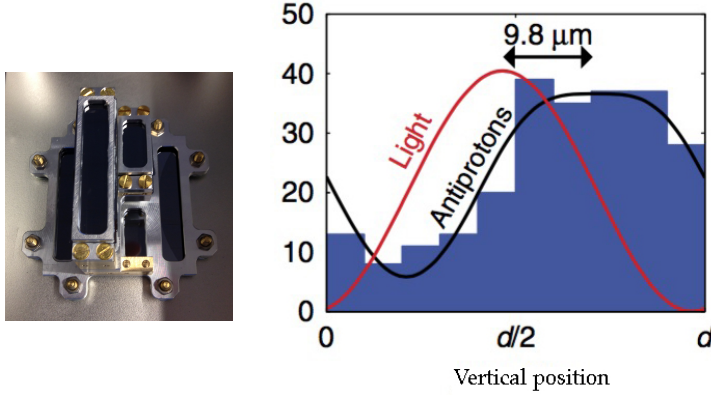


Figure 1.5: *Left: photograph of miniature moiré deflectometer. Right: intensity distribution of reconstructed annihilation vertices (from [6]).*

## 1.2 Fast Annihilation Cryogenic Tracking detector (FACT)

The FACT detector [7] will measure the production and temperature of the  $\bar{H}$  atoms. The operating requirements for this detector are challenging as it needs to identify each of the  $\sim$ thousand annihilations in the 1 ms interval of pulsed  $\bar{H}$  production, operate at 4 K inside a 1 T solenoidal field, and produce less than 10 W of heat. A schematic of the detector is shown in fig. 1.6 (left). The detector consists of two concentric cylindrical layers of scintillating fibers. The scintillating fibers are coupled to clear fibers which transport the scintillation light to 800 silicon photomultipliers. Each silicon photomultiplier signal is connected to an amplifier and a fast discriminator, the outputs of which are sampled continuously by Field Programmable Gate Arrays (FPGAs). The detector is optimised to reconstruct the position of the annihilation vertex along the beam axis, knowledge of which will enable measurements of antihydrogen production, temperature and beam creation. From GEANT4 simulations an annihilation vertex resolution of  $\sigma = 2.1 \text{ mm}$  is expected, which is sufficient for the AEGIS requirements.

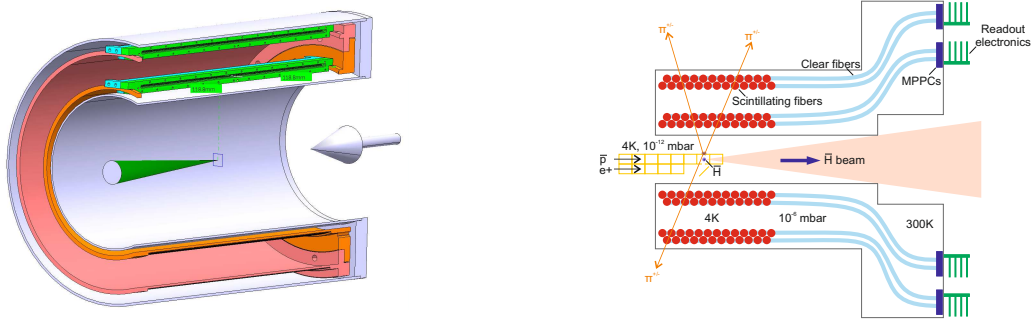


Figure 1.6: *Left: section view of the support structure of the FACT detector. The beam axis is indicated by the arrow and the green cone illustrates the  $\bar{H}$  beam region. Right: layout of the detector (see text).*

The two scintillating fiber layers are mounted on 240 mm long cylindrical support structures (orange and pink cylinders in fig. 1.6). The fibers are located in U shaped grooves. (The mechanical structure was built in the workshop of the Physik-Institut of the University of Zurich.) The blue and green bars are the connectors to couple the scintillating and clear fibers. The scintillating fibers are arranged in loops aligned orthogonally to the beam axis. There are 2 layers at radial distances of 70 mm and 98 mm from the beam axis. Each layer consists of 400 scintillating fibers (1 mm diameter Kuraray SCSF-78M) separated by 0.6 mm, with alternate fibers displaced radially by 0.8 mm. The scintillating light is transported from the cryogenic region to the room temperature readout electronics by means of 2 m long clear fibers (fig. 1.6, right). Particular attention is given to the routing of the



clear fibers to ensure that the minimum bending radius always exceeds 50 mm to avoid light losses. Charged pions (orange lines) from annihilations are reconstructed using the scintillating fiber tracker and extrapolated back to the  $\bar{H}$  formation region to identify the annihilation vertex ( $r, z$  - coordinates). Fig. 1.7 shows the the fibers before (left) and after (middle) being mounted on the support structure.

The scintillation light is guided onto a Hamamatsu Multi-Pixel Photon Counter (MPPC) consisting of 100 Geiger mode Avalanche Photo Diodes (APDs), operating in parallel with a total photosensitive area of 1 mm<sup>2</sup>. The readout electronics is designed to detect continuously the light from the scintillating fibers for the duration of the 100 ms period during which  $\bar{H}$  is produced. The MPPC signal is connected to an amplifier and a fast discriminator read directly by a FPGA. To minimise the heat load to the cryogenic region only the MPPCs are placed inside the vacuum vessel. A plastic connector (developed by the T2K collaboration) is used to couple the clear fibers to the MPPC. The identity of every clear fiber is labelled with coloured glass beads. A photograph of an assembled vacuum feedthrough is shown in fig. 1.7 (right).

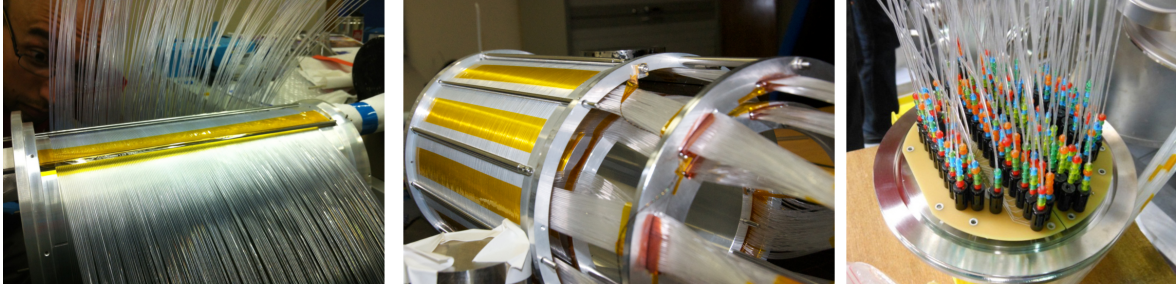


Figure 1.7: *Left and middle: scintillating fibers before and after being mounted on the support structure. The clear fibers emerging from the support structure are organised into groups of 25 fibers and fixed into a circular plate with rectangular slots. Right: clear fibers connected to the MPPCs.*

Fig. 1.8 shows a photograph of the readout electronics. The signals from 96 MPPCs on the vacuum side are routed via the backplane PCB to one of four analogue boards. The readout is supervised by a Xilinx Spartan-6 FPGA development board (bottom left corner). The complete readout system consists of 9 vacuum feedthroughs, 18 backplane PCBs, 67 analogue boards and 16 Spartan-6 development boards.

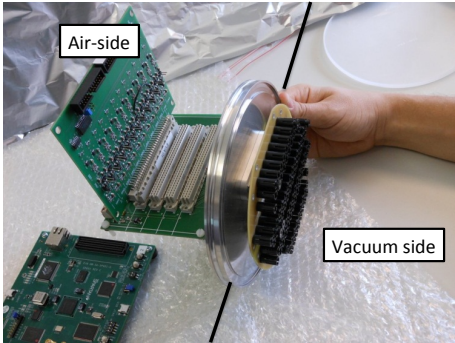


Figure 1.8: *Air and vacuum side electronics for the FACT detector (see text).*

Tests of the plastic scintillating fibers at 4 K have been performed to study the light yield, the decay time and the lifetime of the fibers at cryogenic temperatures. The apparatus to perform this measurement consisted of 3 layers of 1 mm diameter scintillating fibers arranged in loops at the bottom of a liquid helium cryostat. The performance of the scintillating fibers was monitored using

cosmic rays. The rate of events as a function of temperature decreased by  $\approx 10\%$  from room to liquid helium temperature. Examination of the fibers under a microscope after many cycles to 4 K revealed no sign of mechanical damage. The FACT detector was installed in the AEgIS apparatus in 2012.

## References

- [1] G. Drobychev *et al.*, <http://doc.cern.ch/archive/electronic/cern/preprints/spsc/public/spsc-2007-017.pdf>;
- [2] A. Kellerbauer *et al.*, Nucl. Instr. and Meth. **B 266** (2008) 351
- [3] C. Amsler *et al.*, J. of Instrumentation **8** (2013) P02015;  
S. Aghion *et al.* (AEgIS Collaboration), J. of Instrumentation **8** (2013) P08013
- [4] M. Kimura *et al.*, (AEgIS Collaboration), Nucl. Instr. and Meth. in Phys. Res. **A 732** (2013) 325
- [5] G. de Lellis, A. Ereditato, K. Niwa, *Nuclear Emulsions*, C. W. Fabjan and H. Schopper eds., Springer Materials, Landolt-Börnstein Database (<http://www.springermaterials.com>), Springer-Verlag, Heidelberg, 2011
- [6] S. Aghion *et al.* (AEgIS Collaboration), Nature Communications **5** (2014) 4538
- [7] J. Storey *et al.* (AEgIS Collaboration), J. of Instrumentation **10** (2015) C02023